

Pion-Nucleon Sigma Term from Lattice QCD


Rajan Gupta^{1,*} Sungwoo Park^{1,2,†} Martin Hoferichter^{3,‡} Emanuele Mereghetti^{1,§}
Boram Yoon^{4,||} and Tanmoy Bhattacharya^{1,¶}

¹Los Alamos National Laboratory, Theoretical Division T-2, Los Alamos, New Mexico 87545, USA

²Center for Nonlinear Studies, Los Alamos National Laboratory, Los Alamos, New Mexico 87545, USA

³Albert Einstein Center for Fundamental Physics, Institute for Theoretical Physics, University of Bern,
Sidlerstrasse 5, 3012 Bern, Switzerland

⁴Los Alamos National Laboratory, Computer, Computational, and Statistical Sciences Division CCS-7,
Los Alamos, New Mexico 87545, USA

 (Received 9 September 2021; revised 18 October 2021; accepted 27 October 2021; published 7 December 2021)

We present an analysis of the pion-nucleon σ -term $\sigma_{\pi N}$ using six ensembles with $2 + 1 + 1$ -flavor highly improved staggered quark action generated by the MILC Collaboration. The most serious systematic effect in lattice calculations of nucleon correlation functions is the contribution of excited states. We estimate these using chiral perturbation theory (χ PT) and show that the leading contribution to the isoscalar scalar charge comes from $N\pi$ and $N\pi\pi$ states. Therefore, we carry out two analyses of lattice data to remove excited-state contamination, the standard one and a new one including $N\pi$ and $N\pi\pi$ states. We find that the standard analysis gives $\sigma_{\pi N} = 41.9(4.9)$ MeV, consistent with previous lattice calculations, while our preferred χ PT-motivated analysis gives $\sigma_{\pi N} = 59.6(7.4)$ MeV, which is consistent with phenomenological values obtained using πN scattering data. Our data on one physical pion mass ensemble were crucial for exposing this difference, therefore, calculations on additional physical mass ensembles are needed to confirm our result and resolve the tension between lattice QCD and phenomenology.

DOI: [10.1103/PhysRevLett.127.242002](https://doi.org/10.1103/PhysRevLett.127.242002)

Introduction.—This Letter presents results for the pion-nucleon σ -term, $\sigma_{\pi N} \equiv m_{ud} g_S^{u+d} \equiv m_{ud} \langle N(\mathbf{k}, s) | \bar{u}u + \bar{d}d | N(\mathbf{k}, s) \rangle$, calculated in the isospin symmetric limit with $m_{ud} = (m_u + m_d)/2$ as the average of the light quark masses. It is a fundamental parameter of QCD that quantifies the amount of the nucleon mass generated by the u and d quarks. The scalar charge g_S^q is determined from the forward matrix element of the scalar density $\bar{q}q$ between the nucleon state

$$g_S^q = \langle N(\mathbf{k} = 0, s) | Z_S \bar{q}q | N(\mathbf{k} = 0, s) \rangle, \quad (1)$$

where Z_S is the renormalization constant and the nucleon spinor has unit normalization. The connection between g_S^q and the rate of variation of the nucleon mass M_N with the mass of quark with flavor q is given by the Feynman-Hellmann (FH) relation [1–3]

$$\frac{\partial M_N}{\partial m_q} = \langle N(\mathbf{k}, s) | \bar{q}q | N(\mathbf{k}, s) \rangle = g_S^q / Z_S. \quad (2)$$

Published by the American Physical Society under the terms of the [Creative Commons Attribution 4.0 International license](https://creativecommons.org/licenses/by/4.0/). Further distribution of this work must maintain attribution to the author(s) and the published article's title, journal citation, and DOI. Funded by SCOAP³.

The charge g_S^q determines the coupling of the nucleon to the scalar quark current—an important input quantity in the search for physics beyond the standard model (SM), including in direct-detection searches for dark matter [4–8], lepton flavor violation in $\mu \rightarrow e$ conversion in nuclei [9,10], and electric dipole moments [11–14]. In particular, $\sigma_{\pi N}$ is a rare example of a matrix element that, despite the lack of scalar probes in the SM, can still be extracted from phenomenology—via the Cheng-Dashen low-energy theorem [15,16]—and thus defines an important benchmark quantity for lattice QCD.

The low-energy theorem establishes a connection between $\sigma_{\pi N}$ and a pion-nucleon (πN) scattering amplitude, albeit evaluated at unphysical kinematics. Since the one-loop corrections are free of chiral logarithms [17,18], the remaining corrections to the low-energy theorem scale as $\sigma_{\pi N} M_\pi^2 / M_N^2 \approx 1$ MeV, leaving the challenge of controlling the analytic continuation of the isoscalar πN amplitude $\Sigma_{\pi N}$. Stabilizing this extrapolation by means of dispersion relations (and clarifying the relation between $\sigma_{\pi N}$ and $\Sigma_{\pi N}$), Refs. [19–21] found $\sigma_{\pi N} \approx 45$ MeV based on the partial-wave analyses from Refs. [22,23]. More recent partial-wave analyses [24,25] favor higher values, e.g., $\sigma_{\pi N} = 64(8)$ MeV [26]. Similarly, chiral perturbation theory (χ PT) analyses depend crucially on the πN input, with $\sigma_{\pi N}$ prediction varying accordingly [27,28]. Other works

that exploit this relation to πN scattering include Refs. [29–36].

The analytic continuation can be further improved in the framework of Roy-Steiner equations [37–45], whose constraints on $\sigma_{\pi N}$ become most powerful when combined with pionic-atom data on threshold πN scattering [46–50]. Slightly updating the result from Refs. [39,41] to account for the latest data on the pionic hydrogen width [48], one finds $\sigma_{\pi N} = 59.0(3.5)$ MeV. In particular, this determination includes isospin-breaking corrections [51–54] to ensure that $\sigma_{\pi N}$ coincides with its definition in lattice QCD calculations [42]. The difference from Refs. [19–21] traces back to the scattering lengths implied by Refs. [22,23], which are incompatible with the modern pionic-atom data. Independent constraints from experiment are provided by low-energy πN cross sections, including more recent data on both the elastic reactions [55–57] and the charge exchange [58–61], and a global analysis of low-energy data in the Roy-Steiner framework leads to $\sigma_{\pi N} = 58(5)$ MeV [45], in perfect agreement with the pionic-atom result. In contrast, so far, lattice QCD calculations [62–70] have favored low values $\sigma_{\pi N} \approx 40$ MeV (with the exception of Ref. [71]), and it is this persistent tension with phenomenology that we aim to address in this Letter.

There are two ways to calculate $\sigma_{\pi N}$ using lattice QCD, which are called the FH and the direct methods [72]. In the FH method, the nucleon mass is obtained as a function of the bare quark mass m_{ud} (equivalently, M_π^2) from the nucleon two-point correlation function, and its numerical derivative multiplied by m_{ud} gives $\sigma_{\pi N}$. In the direct method, the matrix element of $\bar{u}u + \bar{d}d$ is calculated within the ground-state nucleon. Both methods have their challenges. In the FH method, one needs to calculate the derivative about the physical m_{ud} , which is computationally very demanding. Most calculations extrapolate from heavier masses or fit the data for M_N versus M_π^2 to an ansatz motivated by χ PT and evaluate its derivative at m_{ud} . On the other hand, the signal in the matrix element is noisier since it is obtained from a three-point function with the insertion of the scalar density. In both methods, one has to ensure that all excited-states contamination (ESC) has been removed. Both methods give $\sigma_{\pi N} \approx 40$ MeV—see Fig. 4, review by the Flavour Lattice Averaging Group (FLAG) in 2019 [72], and the two subsequent works [69,70].

Here, we present a new direct-method calculation. Our main message is that $N\pi$ and $N\pi\pi$ excited states, which have not been included in previous lattice calculations, can make a significant contribution. We provide motivation for this effect from heavy baryon χ PT [73,74] and show that including the excited states in fits to the spectral decomposition of the three-point function increases the result by about 50%. Such a change brings the lattice result in agreement with the phenomenological value.

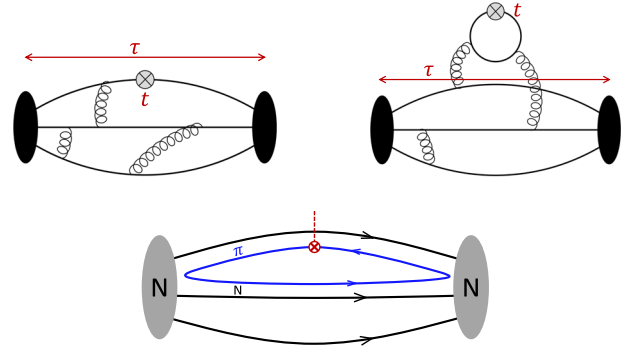


FIG. 1. The upper connected (left) and disconnected (right) diagrams contribute to the three-point function that determines the matrix element of flavor-diagonal scalar operators (shown by symbol \otimes at time slice t) within the nucleon state. The black and gray blobs denote nucleon source and sink, separated by Euclidean time τ . The bottom diagram illustrates that the disconnected diagrams include an $N\pi$ intermediate-state configuration that can give an enhanced contribution.

Lattice methodology and excited states.—The construction of all nucleon two- and three-point correlations functions is carried out using Wilson-clover fermions on six $2 + 1 + 1$ -flavor ensembles generated using the highly improved staggered quark (HISQ) action [75] by the MILC Collaboration [76]. In each of these ensembles, the u - and d -quark masses are degenerate, and the s - and c -quark masses have been tuned to their physical values. Details of the six ensembles at lattice spacings $a \approx 0.12, 0.09,$ and 0.06 fm and $M_\pi \approx 315, 230,$ and 138 MeV are given in Table I (also see Table II and Sec. I in the Supplemental Material [77]). To obtain flavor-diagonal charges g_S^q , two kinds of diagrams, called connected and disconnected and illustrated in Fig. 1, are calculated. The details of the methodology for the calculation of the connected contributions (isovector charges) using this clover-on-HISQ formulation are given in Refs. [118,119] and for the disconnected ones in Ref. [118].

The main focus of the analysis is on controlling the ESC. To this end, we estimate $\sigma_{\pi N}$ using two possible sets of excited-state masses, M_1 and M_2 , given in Table I. These M_i are obtained from simultaneous fits to the zero momentum nucleon two-point $C^{2\text{pt}}$ and three-point $C^{3\text{pt}}$ functions using their spectral decomposition truncated to four and three states, respectively,

$$C^{2\text{pt}}(\tau; \mathbf{k}) = \sum_{i=0}^3 |\mathcal{A}_i(\mathbf{k})|^2 e^{-M_i \tau},$$

$$C_S^{3\text{pt}}(\tau; t) = \sum_{i,j=0}^2 \mathcal{A}_i \mathcal{A}_j^* \langle i | \mathcal{S} | j \rangle e^{-M_i t - M_j (\tau - t)}. \quad (3)$$

Here \mathcal{A}_i are the amplitudes for the creation and annihilation of states by the nucleon interpolating operator used on the

TABLE I. The ground- and excited-state masses M_0 , M_1 , and M_2 , χ^2 of the fit, and the resulting value of the bare isoscalar charge and $\sigma_{\pi N}$ with the two strategies $\{4, 3^*\}$ and $\{4^{N\pi}, 3^*\}$. The second column gives the bare quark mass m_{ud}^{bare} .

Ensemble ID	m_{ud}^{bare} (MeV)	$\{4, 3^*\}$						$\{4^{N\pi}, 3^*\}$					
		M_0 (GeV)	M_1 (GeV)	M_2 (GeV)	$\chi^2/\text{d.o.f.}$	$g_S^{u+d,\text{bare}}$	$\sigma_{\pi N}$ (MeV)	M_0 (GeV)	M_1 (GeV)	M_2 (GeV)	$\chi^2/\text{d.o.f.}$	$g_S^{u+d,\text{bare}}$	$\sigma_{\pi N}$ (MeV)
a12m310	18.7(5)	1.09(1)	1.80(12)	2.7(1)	27/28	8.6(0.6)	160(12)	1.09(1)	1.71(02)	2.6(1)	27/28	8.5(0.5)	160(10)
a12m220	9.9(5)	1.02(1)	1.76(08)	3.0(3)	18/22	10.5(0.5)	104(07)	1.01(1)	1.50(03)	2.6(2)	20/22	11.8(1.0)	117(11)
a09m220	9.4(1)	1.02(1)	1.66(14)	2.4(1)	35/35	10.4(0.8)	98(07)	1.02(1)	1.47(06)	2.3(1)	35/35	11.6(0.9)	109(09)
a09m130	3.5(1)	0.95(1)	1.59(09)	2.8(2)	47/42	11.5(0.8)	40(03)	0.94(1)	1.22(01)	1.8(1)	51/42	15.9(2.3)	55(08)
a06m310	17.2(2)	1.11(1)	1.80(11)	2.9(2)	56/60	10.4(0.7)	179(12)	1.11(1)	1.76(06)	2.8(2)	56/60	10.6(0.6)	182(10)
a06m220	9.1(1)	1.02(1)	1.62(14)	2.5(2)	69/81	10.9(1.0)	98(09)	1.02(1)	1.51(07)	2.3(1)	68/81	11.7(0.8)	106(07)

lattice, $\mathcal{N} = e^{abc}[u^{aT}C\gamma_5(1 + \gamma_4)d^b]u^c$, with color indices $\{a, b, c\}$ and charge conjugation matrix C . The nucleon source-sink separation is labeled by τ and the operator insertion time by t .

The issue of ESC arises because \mathcal{N} couples not only to the ground-state nucleon but to all its excitations, including multihadron states with the same quantum numbers. In the current data, the signal in $C_S^{3\text{pt}}$ extends to $\tau \approx 1.5$ fm, at which source-sink separation the contribution of excited states is significant, as evident from the dependence on $\{\tau, t\}$ in the ratio $\mathcal{R}_S(\tau, t) = C_S^{3\text{pt}}(t, \tau)/C^{2\text{pt}}(\tau)$ shown in Fig. 2. In the limits $t \rightarrow \infty$ and $(\tau - t) \rightarrow \infty$, the ratio $\mathcal{R}_S(\tau, t) \rightarrow g_S$. Fits to $C^{3\text{pt}}$ using Eq. (3) with the key parameters M_i left as free parameters have large fluctuations. We, therefore, remove ESC and extract the ground-state matrix element $\langle 0|S|0\rangle$ using simultaneous fits to $C^{2\text{pt}}$ and $C^{3\text{pt}}$ with common M_i . Statistical precision of the data allowed, without overparametrization, four states in $C^{2\text{pt}}$

(labeled $\{4\}$ or $\{4^{N\pi}\}$) and three states in $C^{3\text{pt}}$ (labeled $\{3^*\}$). We also dropped the unresolved $\langle 2|S|2\rangle$ -term in Eq. (3). Keeping it increases the errors slightly but does not change the values. Using empirical Bayesian priors for M_i and \mathcal{A}_i given in Table V of the Supplemental Material [77], we calculate $\sigma_{\pi N}$ for two plausible but significantly different values of M_1 and M_2 in Table I that give fits with similar χ^2 . A similar strategy has been used in the analysis of axial-vector form factors, where also the $N\pi$ state gives a large contribution as discussed in Refs. [120,121].

Data for $C^{3\text{pt}}$, by Eq. (3), should be (i) symmetric about $\tau/2$ and (ii) converge monotonically in τ for sufficiently large τ , especially when a single excited state dominates. These two conditions are, within errors, satisfied by the data shown in Fig. 2. In the simultaneous fits, M_1 and M_2 are mainly controlled by the four-state fits to $C^{2\text{pt}}$; however, as discussed in Refs. [119,121], there is a large region in $M_{i>0}$ in which the augmented χ^2 of fits with different priors for M_i is essentially the same, i.e., many M_i are plausible. This region covers the towers of positive parity $N\pi, N\pi\pi, \dots$, multihadron states, labeled by increasing relative momentum \mathbf{k} , that can contribute and whose energies start below those of radial excitations. To obtain guidance on which excited states give large contributions to $C^{3\text{pt}}$, we carried out a χ PT analysis.

We study two well-motivated values of M_1 and M_2 for the analysis of $C^{3\text{pt}}$. The “standard” strategy (called the $\{4, 3^*\}$ fit) imposes wide priors on $M_{i>0}$, mostly to stabilize the fits, while the $\{4^{N\pi}, 3^*\}$ fits use narrow-width priors for M_1 centered about the noninteracting energy of the almost degenerate lowest positive parity multihadron states, $N(\mathbf{1})\pi(-\mathbf{1})$ or $N(\mathbf{0})\pi(\mathbf{0})\pi(\mathbf{0})$. Thus, the label $N\pi$ implies that the contribution of both states is included. Details of extracting the M_i from these two four-state fits, $\{4\}$ and $\{4^{N\pi}\}$ to just $C^{2\text{pt}}$, can be found in Ref. [121]. For the $a09m130$ ensemble with $M_\pi = 138$ MeV, the $\{M_1, M_2\}$ are $\{1.59, 2.8\}$ and $\{1.22, 1.8\}$ GeV for the two cases, as shown in Table I. The fits (see Fig. 2) and the χ^2 with respect to $C^{3\text{pt}}$ data are equally good, however, the results for the isoscalar charge g_S^{u+d} differ significantly.

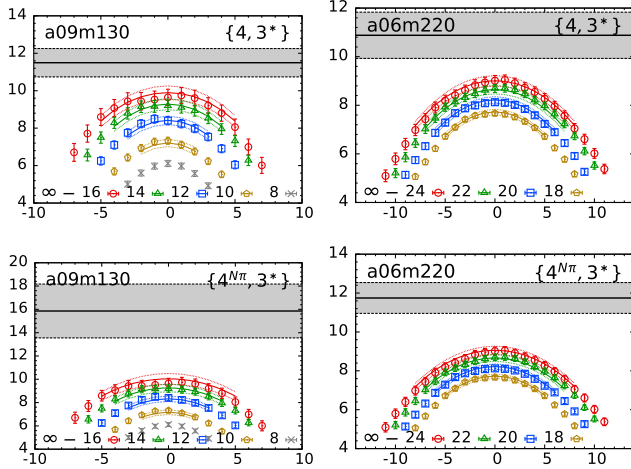


FIG. 2. Results of the $\{4, 3^*\}$ (top row) and $\{4^{N\pi}, 3^*\}$ (bottom row) fits to the sum of the connected and disconnected data plotted versus $(t - \tau/2)/a$ for ensembles $a09m130$ and $a06m220$. Result of the fit is shown by lines of the same color as the data for various τ/a listed in the label, and the $\tau = \infty$ value is given by the gray band.

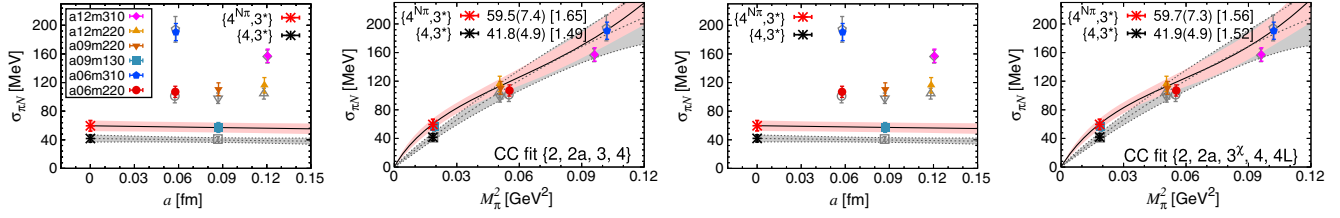


FIG. 3. Data for the σ -term, $\sigma_{\pi N} = m_{ud}g_S^{u+d}$, from the two ESC strategies $\{4, 3^*\}$ (gray) and $\{4^{N\pi}, 3^*\}$ (color) are shown as a function of a and M_π^2 . The two left panels show the chiral-continuum (CC) fit $\{2, 2a, 3, 4\}$ and the two right the CC fit $\{2, 2a, 3^L, 4, 4L\}$ described in the text. The result at $M_\pi = 135$ MeV and $[\chi^2/\text{d.o.f.}]$ of the two fits are given in the legend.

The $\{4, 3^*\}$ fit leads to a result consistent with $\sigma_{\pi N} \approx 40$ MeV, whereas the $\{4^{N\pi}, 3^*\}$ fit gives ≈ 60 MeV. The major difference comes from the disconnected quark loop diagram shown in Fig. 1 and is strongly M_π dependent—the effect of the $N\pi$ states is hard to resolve in the $M_\pi \approx 315$ MeV data, debatable in the 230 MeV data, and clear in the $M_\pi = 138$ MeV data.

It is important to point out that the values of M_1 and M_2 used in both fit strategies are an effective bundling of the many excited states that contribute into two. In fact, as mentioned above, many combinations of M_1 and M_2 between $\{4, 3^*\}$ and $\{4^{N\pi}, 3^*\}$ (see Table I) give fits with equally good χ^2 values. Reference [121] showed that, for $\tau \gtrsim 1.0$ fm and for both fit strategies, the dominant ESC in $C^{3\text{pt}}$ comes from the first excited state. Thus, operationally, our two results for $\sigma_{\pi N}$ should be regarded as what happens if the first “effective” excited state has $M_1 \approx 1220$ MeV (motivated by χ PT and corresponding to the lowest theoretically possible states $N\pi$ or $N\pi\pi$) versus 1600 MeV obtained from the standard fit to the two-point function. To further resolve all the excited states that contribute significantly and their energies in a finite box requires much higher precision data on additional $M_\pi \approx 135$ MeV ensembles. In short, while our $\{4^{N\pi}, 3^*\}$ analysis reconciles the lattice and the phenomenological values, it also calls for validation in future calculations.

Excited states in χ PT.—The contributions of low-momentum $N\pi$ and $N\pi\pi$ states to $C^{2\text{pt}}$ and $C^{3\text{pt}}$ can be studied in χ PT [122–129], a low-energy effective field theory of QCD that provides a systematic expansion of $\mathcal{R}_S(\tau, t)$ in powers of Q/Λ_χ , where Q denotes a low-energy scale of order of the pion mass, $Q \in \{M_\pi, t^{-1}, (\tau - t)^{-1}\}$, while $\Lambda_\chi \approx 1$ GeV is the typical scale of QCD. In contrast to the isovector scalar charge considered in Ref. [124], we find large contributions from the $N(\mathbf{k})\pi(-\mathbf{k})$ and $N(\mathbf{0})\pi(\mathbf{k})\pi(-\mathbf{k})$ states, which can give up to 30% corrections to \mathcal{R}_S and thus affect the extraction of g_S^{u+d} and $\sigma_{\pi N}$ in a significant way.

The diagrams contributing to \mathcal{R}_S are shown in Fig. 5 of the Supplemental Material [77], where we assume $\mathcal{N}(x)$ to be a local nucleon source with well-defined transformation properties under chiral symmetry. The chiral representation of this class of sources has been derived in Refs. [122,123,130].

Details of the calculation at next-to-next-to-leading order (N^2 LO) in χ PT and the expansion of \mathcal{N} in terms of heavy nucleon and pion fields are summarized in the Supplemental Material [77], Sec. II. The crucial observation is that the isoscalar scalar source couples strongly to two pions, so that loop diagrams with the scalar source emitting two pions, which are consequently absorbed by the nucleon, are suppressed by only one chiral order Q/Λ_χ . These diagrams have both $N\pi$ and $N\pi\pi$ cuts, which give rise to ESC to Euclidean Green’s functions. A second important effect is that the next-to-leading-order (NLO) couplings of the nucleon to two pions, parameterized in χ PT by the low-energy constants (LECs) $c_{1,2,3}$, are sizable, reflecting the enhancement by degrees of freedom related to the $\Delta(1232)$. When the pions couple to the isoscalar source, these couplings give rise to large N^2 LO corrections that are dominated by $N\pi\pi$ excited states and have the same sign as the NLO correction. Since, in the isospin-symmetric limit, the isovector scalar source does not couple to two pions, the NLO diagrams and the N^2 LO diagrams proportional to $c_{1,2,3}$ do not contribute to the isovector three-point function, whose leading ESC arises at $\mathcal{O}(Q^2/\Lambda_\chi^2)$. A detailed analysis showing that the functional form of the ESC predicted by χ PT matches the lattice data and fits for sufficiently large time separations τ is given in the Supplemental Material [77], Sec. II. In particular, the NLO and N^2 LO ESC can each reduce $\sigma_{\pi N}$ at a level of 10 MeV, thus explaining the $\{4^{N\pi}, 3^*\}$ fits, i.e., a larger value when ESC is taken into account.

Analysis of lattice data.—Examples of fits with strategies $\{4, 3^*\}$ and $\{4^{N\pi}, 3^*\}$ to remove ESC and obtain $g_S^{u+d,\text{bare}}$ are shown in Fig. 2 and the results are summarized in Table I. The final results are obtained from fits to the sum of the connected and disconnected contributions. These values overlap in all cases with the sum of estimates from separate fits to $g_S^{u+d,\text{conn}}$ and g_S^{2l} . From the separate fits, we infer that most of the difference between the two ESC strategies comes from the disconnected diagrams, which we interpret as due to the $N\pi/N\pi\pi$ contributions through quark-level diagrams such as shown in Fig. 1.

Figure 3 shows data for $\sigma_{\pi N} = m_{ud}^{\text{bare}}g_S^{u+d,\text{bare}}$ as a function of a and M_π^2 . The chiral-continuum extrapolation is carried out using the N^2 LO χ PT expression [41]

$$\sigma_{\pi N} = (d_2 + d_2^a)M_\pi^2 + d_3M_\pi^3 + d_4M_\pi^4 + d_{4L}M_\pi^4 \log \frac{M_\pi^2}{M_N^2}. \quad (4)$$

The d_i in χ PT (henceforth labeled d_i^{χ}) are given in the Supplemental Material [77] [Eq. (14)] and evaluated with $M_N = 0.939$ GeV, $g_A = 1.276$, and $F_\pi = 92.3$ MeV. Neglected finite-volume corrections can also be estimated in χ PT, see Sec. II in the Supplemental Material [77] and Refs. [119,131], indicating a correction of less than 1 MeV for the $a09m130$ ensemble.

Figure 3 shows two chiral fits based on the N^2 LO χ PT expression for $\sigma_{\pi N}$. The $\{2, 2a, 3, 4\}$ fit keeps terms proportional to $\{d_2, d_2^a, d_3, d_4\}$ with all coefficients free. In the $\{2, 2a, 3^\chi, 4, 4L\}$ fit we use the χ PT value for $d_3 = d_3^\chi$, which does not involve any LECs, and include the d_{4L} -term. Each panel also shows the six data points obtained with the $\{4, 3^*\}$ and $\{4^{N\pi}, 3^*\}$ strategies and the fits to them. In each fit d_2^a comes out consistent with zero.

The results for $\sigma_{\pi N}$ at the physical point $M_\pi = 135$ MeV from the various fits are essentially given by the $a09m130$ point. We have neglected a correction due to flavor mixing inherent in Wilson-clover fermions since it is small, as shown in the Supplemental Material [77], Sec. IV. Our final result, $\sigma_{\pi N} = 59.6(7.4)$, is the average of results from the $\{2, 2a, 3, 4\}$ and $\{2, 2a, 3^\chi, 4, 4L\}$ fits to the $\{4^{N\pi}, 3^*\}$ data given in Fig. 3, which overlap. In the Supplemental Material [77] (Sec. II), we consider more constrained fit variants, which show that the fit coefficients of the M_π^2 and $M_\pi^4 \log M_\pi^2$ terms are also broadly consistent with their χ PT prediction.

Conclusions.—Results for $\sigma_{\pi N}$ were reviewed by FLAG in 2019 [72], and there have been two new calculations since as summarized in Sec. V of the Supplemental Material [77] and shown in Fig. 4. The ETM Collaboration [69], using the direct method on one physical mass $2 + 1 + 1$ -flavor twisted mass clover-improved ensemble, obtained $\sigma_{\pi N} = 41.6(3.8)$ MeV; the BMW Collaboration using the FH method and 33 ensembles of $1 + 1 + 1 + 1$ -flavor Wilson-clover fermions [70], but all with $M_\pi > 199$ MeV, find $\sigma_{\pi N} = 37.4(5.1)$ MeV. The χ PT analysis of the impact of low-lying excited $N\pi$ states in the FH and direct methods is the same, and as shown in Fig. 3, it mainly affects the behavior for $M_\pi \lesssim 135$ MeV. Our work indicates that previous lattice calculations give the lower value $\sigma_{\pi N} \approx 40$ MeV because in the FH analysis [70] the fit ansatz (Taylor or Padé) parameters are determined using $M_\pi \geq 199$ MeV data, and in the direct method, the $N\pi/N\pi\pi$ states have not been included when extracting the ground-state matrix element [69].

To conclude, a χ PT analysis shows that the low-lying $N\pi$ and $N\pi\pi$ states can make a significant contribution to $g_S^{\mu+d}$. Including these states in our analysis (the $\{4^{N\pi}, 3^*\}$ strategy) gives $\sigma_{\pi N} = 59.6(7.4)$ MeV, whereas the standard

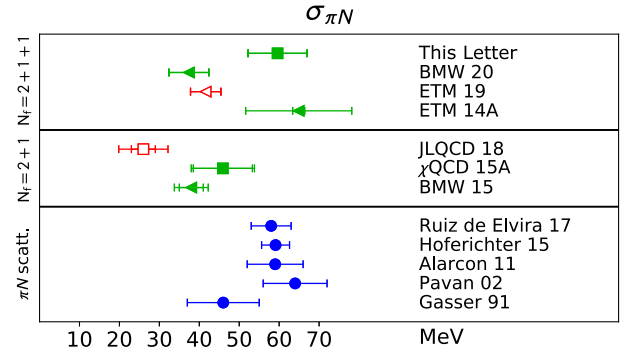


FIG. 4. Results for $\sigma_{\pi N} = m_{ud}g_S^{\mu+d}$ from $2 + 1$ - and $2 + 1 + 1$ -flavor lattice calculations. The BMW 20 result from $1 + 1 + 1 + 1$ -flavor lattices is listed along with the other $2 + 1 + 1$ -flavor calculations for brevity. Following the FLAG conventions, determinations via the direct approach are indicated by squares and the FH method by triangles. Also, the symbols used for lattice estimates that satisfy the FLAG criteria for inclusion in averages are filled green, and those not included are open red. The references from which lattice results have been taken are as follows: JLQCD 18 [68], χ QCD 15A [65], BMW 15 [64], ETM 14A [71], ETM 19 [69], and BMW 20 [70]. Phenomenological estimates using πN scattering data (blue filled circles) are from Gasser *et al.* 91 [20], Pavan *et al.* 02 [26], Alarcón *et al.* 11 [28], Hoferichter *et al.* 15 [39], and Ruiz de Elvira *et al.* 17 [45].

analysis ($\{4, 3^*\}$ strategy) gives $\sigma_{\pi N} = 41.9(4.9)$ MeV consistent with previous analyses [72]. These chiral fits are shown in Fig. 3. Since the $\{4, 3^*\}$ and $\{4^{N\pi}, 3^*\}$ strategies to remove ESC are not distinguished by the χ^2 of the fits, we provide a detailed N^2 LO χ PT analysis of ESC, which reveals sizable corrections consistent with the $\{4^{N\pi}, 3^*\}$ analysis, restoring agreement with phenomenology. Since the effect of the $N\pi$ and $N\pi\pi$ states becomes significant near $M_\pi = 135$ MeV, further work on physical mass ensembles is needed to validate our result and to increase the precision in the extraction of the nucleon isoscalar scalar charge.

We thank O. Bär, L. Lellouch, and A. Walker-Loud for comments on the manuscript and the MILC collaboration for providing the $2 + 1 + 1$ -flavor HISQ lattices. The calculations used the CHROMA software suite [132]. This research used resources at (i) the National Energy Research Scientific Computing Center, a DOE Office of Science User Facility supported by the Office of Science of the U.S. Department of Energy under Award No. DE-AC02-05CH11231; (ii) the Oak Ridge Leadership Computing Facility, which is a DOE Office of Science User Facility supported under Award No. DE-AC05-00OR22725 and was awarded through the ALCC program project LGT107; (iii) the USQCD Collaboration, which is funded by the Office of Science of the U.S. Department of Energy; and (iv) Institutional Computing at Los Alamos National Laboratory. T. B. and R. G. were partly supported by the U.S. Department of Energy, Office of Science, Office of High Energy Physics

under Award No. DE-AC52-06NA25396. T.B., R.G., E.M., S.P., and B.Y. were partly supported by the LANL LDRD program, and S.P. was supported by the Center for Nonlinear Studies. M.H. was supported by the Swiss National Science Foundation (Project No. PCEFP2_181117).

*rajan@lanl.gov
 †sungwoo@jlab.org
 ‡hoferichter@itp.unibe.ch
 §emereghetti@lanl.gov
 ‖boram@lanl.gov
 ¶tanmoy@lanl.gov

- [1] H. Hellman, *Einführung in die Quantenchemie* (Franz Deuticke, Leipzig und Wein, 1937).
- [2] R. P. Feynman, *Phys. Rev.* **56**, 340 (1939).
- [3] J. Gasser and A. Zepeda, *Nucl. Phys.* **B174**, 445 (1980).
- [4] A. Bottino, F. Donato, N. Fornengo, and S. Scopel, *Astropart. Phys.* **13**, 215 (2000).
- [5] A. Bottino, F. Donato, N. Fornengo, and S. Scopel, *Astropart. Phys.* **18**, 205 (2002).
- [6] J. R. Ellis, K. A. Olive, and C. Savage, *Phys. Rev. D* **77**, 065026 (2008).
- [7] A. Crivellin, M. Hoferichter, and M. Procura, *Phys. Rev. D* **89**, 054021 (2014).
- [8] M. Hoferichter, P. Klos, J. Menéndez, and A. Schwenk, *Phys. Rev. Lett.* **119**, 181803 (2017).
- [9] V. Cirigliano, R. Kitano, Y. Okada, and P. Tuzon, *Phys. Rev. D* **80**, 013002 (2009).
- [10] A. Crivellin, M. Hoferichter, and M. Procura, *Phys. Rev. D* **89**, 093024 (2014).
- [11] J. Engel, M. J. Ramsey-Musolf, and U. van Kolck, *Prog. Part. Nucl. Phys.* **71**, 21 (2013).
- [12] J. de Vries and Ulf-G. Meißner, *Int. J. Mod. Phys. E* **25**, 1641008 (2016).
- [13] J. de Vries, E. Mereghetti, C.-Y. Seng, and A. Walker-Loud, *Phys. Lett. B* **766**, 254 (2017).
- [14] N. Yamanaka, B. K. Sahoo, N. Yoshinaga, T. Sato, K. Asahi, and B. P. Das, *Eur. Phys. J. A* **53**, 54 (2017).
- [15] T. P. Cheng and R. F. Dashen, *Phys. Rev. Lett.* **26**, 594 (1971).
- [16] L. S. Brown, W. J. Pardee, and R. D. Peccei, *Phys. Rev. D* **4**, 2801 (1971).
- [17] V. Bernard, N. Kaiser, and Ulf-G. Meißner, *Phys. Lett. B* **389**, 144 (1996).
- [18] T. Becher and H. Leutwyler, *J. High Energy Phys.* **06** (2001) 017.
- [19] J. Gasser, H. Leutwyler, M. P. Locher, and M. E. Sainio, *Phys. Lett. B* **213**, 85 (1988).
- [20] J. Gasser, H. Leutwyler, and M. E. Sainio, *Phys. Lett. B* **253**, 252 (1991).
- [21] J. Gasser, H. Leutwyler, and M. E. Sainio, *Phys. Lett. B* **253**, 260 (1991).
- [22] R. Koch and E. Pietarinen, *Nucl. Phys.* **A336**, 331 (1980).
- [23] G. Höhler, *Methods and Results of Phenomenological Analyses*, edited by H. Schopper, Landolt-Boernstein—Group I Elementary Particles, Nuclei and Atoms Vol. 9b2 (Springer-Verlag, Berlin, Heidelberg, 1983).
- [24] R. A. Arndt, W. J. Briscoe, I. I. Strakovsky, and R. L. Workman, *Phys. Rev. C* **74**, 045205 (2006).
- [25] R. L. Workman, R. A. Arndt, W. J. Briscoe, M. W. Paris, and I. I. Strakovsky, *Phys. Rev. C* **86**, 035202 (2012).
- [26] M. M. Pavan, I. I. Strakovsky, R. L. Workman, and R. A. Arndt, *PiN Newslett.* **16**, 110 (2002), <https://arxiv.org/abs/hep-ph/0111066>.
- [27] N. Fettes and Ulf-G. Meißner, *Nucl. Phys.* **A676**, 311 (2000).
- [28] J. M. Alarcón, J. Martin Camalich, and J. A. Oller, *Phys. Rev. D* **85**, 051503(R) (2012).
- [29] R. Koch, *Z. Phys. C* **15**, 161 (1982).
- [30] T. E. O. Ericson, *Phys. Lett. B* **195**, 116 (1987).
- [31] G. Höhler, *PiN Newslett.* **2**, 1 (1990), <https://gwu.edu/Newsletters/PiN-Newsletter-02.pdf>.
- [32] M. G. Olsson, *Phys. Lett. B* **482**, 50 (2000).
- [33] G. E. Hite, W. B. Kaufmann, and R. J. Jacob, *Phys. Rev. C* **71**, 065201 (2005).
- [34] M. Hadzimehmedovic, H. Osmanovic, and J. Stahov, *eConf C070910*, 234 (2007), <https://www.slac.stanford.edu/econf/C070910/PDF/234.pdf>.
- [35] J. Stahov, H. Clement, and G. J. Wagner, *Phys. Lett. B* **726**, 685 (2013).
- [36] E. Matsinos and G. Rasche, *Nucl. Phys.* **A927**, 147 (2014).
- [37] C. Ditsche, M. Hoferichter, B. Kubis, and Ulf-G. Meißner, *J. High Energy Phys.* **06** (2012) 043.
- [38] M. Hoferichter, C. Ditsche, B. Kubis, and Ulf-G. Meißner, *J. High Energy Phys.* **06** (2012) 063.
- [39] M. Hoferichter, J. Ruiz de Elvira, B. Kubis, and Ulf-G. Meißner, *Phys. Rev. Lett.* **115**, 092301 (2015).
- [40] M. Hoferichter, J. Ruiz de Elvira, B. Kubis, and Ulf-G. Meißner, *Phys. Rev. Lett.* **115**, 192301 (2015).
- [41] M. Hoferichter, J. Ruiz de Elvira, B. Kubis, and Ulf-G. Meißner, *Phys. Rep.* **625**, 1 (2016).
- [42] M. Hoferichter, J. Ruiz de Elvira, B. Kubis, and Ulf-G. Meißner, *Phys. Lett. B* **760**, 74 (2016).
- [43] M. Hoferichter, B. Kubis, J. Ruiz de Elvira, H.-W. Hammer, and Ulf-G. Meißner, *Eur. Phys. J. A* **52**, 331 (2016).
- [44] D. Siemens, J. Ruiz de Elvira, E. Epelbaum, M. Hoferichter, H. Krebs, B. Kubis, and Ulf-G. Meißner, *Phys. Lett. B* **770**, 27 (2017).
- [45] J. Ruiz de Elvira, M. Hoferichter, B. Kubis, and Ulf-G. Meißner, *J. Phys. G* **45**, 024001 (2018).
- [46] Th. Strauch, F. D. Amaro, D. F. Anagnostopoulos, P. Bühler, D. S. Covita, H. Gorke *et al.*, *Eur. Phys. J. A* **47**, 88 (2011).
- [47] M. Hennebach, D. F. Anagnostopoulos, A. Dax, H. Fuhrmann, D. Gotta, A. Gruber *et al.*, *Eur. Phys. J. A* **50**, 190 (2014); **55**, 24(E) (2019).
- [48] A. Hirtl, D. F. Anagnostopoulos, D. S. Covita, H. Fuhrmann, H. Gorke, D. Gotta *et al.*, *Eur. Phys. J. A* **57**, 70 (2021).
- [49] V. Baru, C. Hanhart, M. Hoferichter, B. Kubis, A. Nogga, and D. R. Phillips, *Phys. Lett. B* **694**, 473 (2011).
- [50] V. Baru, C. Hanhart, M. Hoferichter, B. Kubis, A. Nogga, and D. R. Phillips, *Nucl. Phys.* **A872**, 69 (2011).
- [51] J. Gasser, M. A. Ivanov, E. Lipartia, M. Mojžiš, and A. Rusetsky, *Eur. Phys. J. C* **26**, 13 (2002).
- [52] M. Hoferichter, B. Kubis, and Ulf-G. Meißner, *Phys. Lett. B* **678**, 65 (2009).

- [53] M. Hoferichter, B. Kubis, and Ulf-G. Meißner, *Nucl. Phys.* **A833**, 18 (2010).
- [54] M. Hoferichter, V. Baru, C. Hanhart, B. Kubis, A. Nogga, and D. R. Phillips, *Proc. Sci.*, CD12 (2013) 093.
- [55] J. T. Brack, R. A. Ristinen, J. J. Kraushaar, R. A. Loveman, R. J. Peterson, G. R. Smith, D. R. Gill, D. F. Ottewell, M. E. Seviar, R. P. Trelle, E. L. Mathie, N. Grion, and R. Rui, *Phys. Rev. C* **41**, 2202 (1990).
- [56] Ch. Joram, M. Metzler, J. Jaki, W. Kluge, H. Matthäy, R. Wieser, B. M. Barnett, H. Clement, S. Krell, and G. J. Wagner, *Phys. Rev. C* **51**, 2144 (1995).
- [57] H. Denz, P. Amaudruz, J. T. Brack, J. Breitschopf, P. Camerini, J. L. Clark *et al.*, *Phys. Lett. B* **633**, 209 (2006).
- [58] E. Frlež, D. Počanić, K. A. Assamagan, J. P. Chen, K. J. Keeter, R. M. Marshall, R. C. Minehart, L. C. Smith, G. E. Dodge, S. S. Hanna, B. H. King, and J. N. Knudson, *Phys. Rev. C* **57**, 3144 (1998).
- [59] L. D. Isenhower, T. Black, B. M. Brooks, A. D. Brown, K. Graessle *et al.*, *PiN Newslett.* **15**, 292 (1999), <https://gwadac.phys.gwu.edu/Newsletters/PiN-Newsletter-15.pdf>.
- [60] Y. Jia, T. P. Goringe, M. D. Hasinoff, M. A. Kovash, M. Ojha, M. M. Pavan, S. Tripathi, and P. A. Żołnierczuk, *Phys. Rev. Lett.* **101**, 102301 (2008).
- [61] D. Mekterović, I. Supek, V. Abaev, V. Bekrenev, C. Bircher, W. J. Briscoe *et al.* (Crystal Ball Collaboration), *Phys. Rev. C* **80**, 055207 (2009).
- [62] S. Dürr, Z. Fodor, T. Hemmert, C. Hoelbling, J. Frison, S. D. Katz, S. Krieg, T. Kurth, L. Lellouch, T. Lippert, A. Portelli, A. Ramos, A. Schäfer, and K. K. Szabó (BMWc Collaboration), *Phys. Rev. D* **85**, 014509 (2012); **93**, 039905(E) (2016).
- [63] G. S. Bali, P. C. Bruns, S. Collins, M. Deka, B. Gläble, M. Göckeler *et al.* (QCDSF Collaboration), *Nucl. Phys.* **B866**, 1 (2013).
- [64] S. Dürr, Z. Fodor, C. Hoelbling, S. D. Katz, S. Krieg, L. Lellouch, T. Lippert, T. Metivet, A. Portelli, K. K. Szabo, C. Torrero, B. C. Toth, and L. Varnhorst (Budapest-Marseille-Wuppertal Collaboration), *Phys. Rev. Lett.* **116**, 172001 (2016).
- [65] Y.-B. Yang, A. Alexandru, T. Draper, J. Liang, and K.-F. Liu (χ QCD Collaboration), *Phys. Rev. D* **94**, 054503 (2016).
- [66] A. Abdel-Rehim, C. Alexandrou, M. Constantinou, K. Hadjiyiannakou, K. Jansen, C. Kallidonis, G. Koutsou, and A. Vaquero Avilés-Casco (ETM Collaboration), *Phys. Rev. Lett.* **116**, 252001 (2016).
- [67] G. S. Bali, S. Collins, D. Richtmann, A. Schäfer, W. Söldner, and A. Sternbeck (RQCD Collaboration), *Phys. Rev. D* **93**, 094504 (2016).
- [68] N. Yamanaka, S. Hashimoto, T. Kaneko, and H. Ohki (JLQCD Collaboration), *Phys. Rev. D* **98**, 054516 (2018).
- [69] C. Alexandrou, S. Bacchio, M. Constantinou, J. Finkenrath, K. Hadjiyiannakou, K. Jansen, G. Koutsou, and A. Vaquero Avilés-Casco (ETM Collaboration), *Phys. Rev. D* **102**, 054517 (2020).
- [70] Sz. Borsanyi, Z. Fodor, C. Hoelbling, L. Lellouch, K. K. Szabo, C. Torrero, and L. Varnhorst (BMWc), [arXiv:2007.03319](https://arxiv.org/abs/2007.03319).
- [71] C. Alexandrou, V. Drach, K. Jansen, C. Kallidonis, and G. Koutsou, *Phys. Rev. D* **90**, 074501 (2014).
- [72] S. Aoki, Y. Aoki, D. Bečirević, T. Blum, G. Colangelo, S. Collins *et al.* (Flavour Lattice Averaging Group), *Eur. Phys. J. C* **80**, 113 (2020).
- [73] E. E. Jenkins and A. V. Manohar, *Phys. Lett. B* **255**, 558 (1991).
- [74] V. Bernard, N. Kaiser, J. Kambor, and Ulf-G. Meißner, *Nucl. Phys.* **B388**, 315 (1992).
- [75] E. Follana, Q. Mason, C. Davies, K. Hornbostel, G. P. Lepage, J. Shigemitsu, H. Trotter, and K. Wong (HPQCD, UKQCD Collaboration), *Phys. Rev. D* **75**, 054502 (2007).
- [76] A. Bazavov, C. Bernard, J. Komijani, C. DeTar, L. Levkova, W. Freeman, S. Gottlieb, R. Zhou, U. M. Heller, J. E. Hetrick, J. Laiho, J. Osborn, R. L. Sugar, D. Toussaint, and R. S. Van de Water (MILC Collaboration), *Phys. Rev. D* **87**, 054505 (2013).
- [77] See Supplemental Material at <http://link.aps.org/supplemental/10.1103/PhysRevLett.127.242002> for details of the lattice parameters and analyses, derivations and analyses using χ PT, and chiral fits to nucleon mass, which includes Refs. [78–117].
- [78] C. Alexandrou and C. Kallidonis, *Phys. Rev. D* **96**, 034511 (2017).
- [79] L. Alvarez-Ruso, T. Ledwig, J. Martin Camalich, and M. J. Vicente-Vacas, *Phys. Rev. D* **88**, 054507 (2013).
- [80] G. S. Bali, S. Collins, and A. Schäfer, *Comput. Phys. Commun.* **181**, 1570 (2010).
- [81] G. S. Bali, L. Barca, S. Collins, M. Gruber, M. Löffler, A. Schäfer, W. Söldner, P. Wein, S. Weishäupl, and T. Wurm (RQCD Collaboration), *J. High Energy Phys.* **05** (2020) 126.
- [82] S. R. Beane, *Phys. Rev. D* **70**, 034507 (2004).
- [83] T. Becher and H. Leutwyler, *Eur. Phys. J. C* **9**, 643 (1999).
- [84] V. Bernard, N. Kaiser, and Ulf-G. Meißner, *Int. J. Mod. Phys. E* **04**, 193 (1995).
- [85] T. Bhattacharya, R. Gupta, W. Lee, S. R. Sharpe, and J. M. S. Wu, *Phys. Rev. D* **73**, 034504 (2006).
- [86] T. Blum, T. Izubuchi, and E. Shintani, *Phys. Rev. D* **88**, 094503 (2013).
- [87] B. Borasoy and Ulf-G. Meißner, *Ann. Phys. (N.Y.)* **254**, 192 (1997).
- [88] Y.-H. Chen, D.-L. Yao, and H. Q. Zheng, *Phys. Rev. D* **87**, 054019 (2013).
- [89] G. Colangelo and S. Dürr, *Eur. Phys. J. C* **33**, 543 (2004).
- [90] J. Gasser, M. E. Sainio, and A. Švarc, *Nucl. Phys.* **B307**, 779 (1988).
- [91] S. Gusken, U. Low, K. H. Mutter, R. Sommer, A. Patel, and K. Schilling, *Phys. Lett. B* **227**, 266 (1989).
- [92] R. Horsley, Y. Nakamura, H. Perlt, D. Pleiter, P. E. L. Rakow, G. Schierholz, A. Schiller, H. Stuben, F. Winter, and J. M. Zanotti (QCDSF-UKQCD Collaboration), *Phys. Rev. D* **85**, 034506 (2012).
- [93] K.-I. Ishikawa, N. Ishizuka, T. Izubuchi, D. Kadoh, K. Kanaya, Y. Kuramashi *et al.* (PACS-CS Collaboration), *Phys. Rev. D* **80**, 054502 (2009).
- [94] P. M. Junnarkar and A. Walker-Loud, *Phys. Rev. D* **87**, 114510 (2013).
- [95] J. Kambor and M. Mojžiš, *J. High Energy Phys.* **04** (1999) 031.
- [96] X.-L. Ren, X.-Z. Ling, and L.-S. Geng, *Phys. Lett. B* **783**, 7 (2018).

- [97] M. F. M. Lutz, R. Bavontaweepanya, C. Kobdaj, and K. Schwarz, *Phys. Rev. D* **90**, 054505 (2014).
- [98] M. F. M. Lutz, Y. Heo, and X.-Y. Guo, *Nucl. Phys.* **A977**, 146 (2018).
- [99] J. Martin Camalich, L. S. Geng, and M. J. Vicente-Vacas, *Phys. Rev. D* **82**, 074504 (2010).
- [100] J. A. McGovern and M. C. Birse, *Phys. Lett. B* **446**, 300 (1999).
- [101] J. A. McGovern and M. C. Birse, *Phys. Rev. D* **74**, 097501 (2006).
- [102] Ulf-G. Meißner and S. Steininger, *Phys. Lett. B* **419**, 403 (1998).
- [103] H. Ohki, H. Fukaya, S. Hashimoto, T. Kaneko, H. Matsufuru, J. Noaki, T. Onogi, E. Shintani, and N. Yamada, *Phys. Rev. D* **78**, 054502 (2008).
- [104] H. Ohki, K. Takeda, S. Aoki, S. Hashimoto, T. Kaneko, H. Matsufuru, J. Noaki, and T. Onogi (JLQCD Collaboration), *Phys. Rev. D* **87**, 034509 (2013).
- [105] M. Procura, B. U. Musch, T. Wollenweber, T. R. Hemmert, and W. Weise, *Phys. Rev. D* **73**, 114510 (2006).
- [106] X.-L. Ren, L. S. Geng, J. Martin Camalich, J. Meng, and H. Toki, *J. High Energy Phys.* **12** (2012) 073.
- [107] X.-L. Ren, L.-S. Geng, and J. Meng, *Phys. Rev. D* **91**, 051502(R) (2015).
- [108] X.-L. Ren, L. Alvarez-Ruso, L.-S. Geng, T. Ledwig, J. Meng, and M. J. Vicente-Vacas, *Phys. Lett. B* **766**, 325 (2017).
- [109] M. R. Schindler, D. Djukanovic, J. Gegelia, and S. Scherer, *Phys. Lett. B* **649**, 390 (2007).
- [110] M. R. Schindler, D. Djukanovic, J. Gegelia, and S. Scherer, *Nucl. Phys.* **A803**, 68 (2008); **A1010**, 122175 (E) (2021).
- [111] P. E. Shanahan, A. W. Thomas, and R. D. Young, *Phys. Rev. D* **87**, 074503 (2013).
- [112] S. Steininger, Ulf-G. Meißner, and N. Fettes, *J. High Energy Phys.* **09** (1998) 008.
- [113] A. Walker-Loud, *Proc. Sci.*, CD12 (2013) 017.
- [114] A. Walker-Loud, H.-W. Lin, D. G. Richards, R. G. Edwards, M. Engelhardt, G. T. Fleming *et al.*, *Phys. Rev. D* **79**, 054502 (2009).
- [115] A. Walker-Loud, *Proc. Sci.*, LATTICE2008 (2008) 005.
- [116] R. D. Young and A. W. Thomas, *Phys. Rev. D* **81**, 014503 (2010).
- [117] P. A. Zyla, R. M. Barnett, J. Beringer, O. Dahl, D. A. Dwyer, D. E. Groom *et al.* (Particle Data Group), *Prog. Theor. Exp. Phys.* **2020**, 083C01 (2020).
- [118] T. Bhattacharya, V. Cirigliano, S. D. Cohen, R. Gupta, A. Joseph, H.-W. Lin, and B. Yoon (PNDME Collaboration), *Phys. Rev. D* **92**, 094511 (2015).
- [119] R. Gupta, Y.-C. Jang, B. Yoon, H.-W. Lin, V. Cirigliano, and T. Bhattacharya, *Phys. Rev. D* **98**, 034503 (2018).
- [120] Y.-C. Jang, R. Gupta, B. Yoon, and T. Bhattacharya, *Phys. Rev. Lett.* **124**, 072002 (2020).
- [121] S. Park, R. Gupta, B. Yoon, S. Mondal, T. Bhattacharya, Y.-C. Jang, B. Joó, and F. Winter (Nucleon Matrix Elements Collaboration), [arXiv:2103.05599](https://arxiv.org/abs/2103.05599).
- [122] O. Bär, *Phys. Rev. D* **92**, 074504 (2015).
- [123] B. C. Tiburzi, *Phys. Rev. D* **91**, 094510 (2015).
- [124] O. Bär, *Phys. Rev. D* **94**, 054505 (2016).
- [125] O. Bär, *Phys. Rev. D* **95**, 034506 (2017).
- [126] O. Bär, *Phys. Rev. D* **97**, 094507 (2018).
- [127] O. Bär, *Phys. Rev. D* **99**, 054506 (2019).
- [128] O. Bär, *Phys. Rev. D* **100**, 054507 (2019).
- [129] O. Bär and H. Čolić, *Phys. Rev. D* **103**, 114514 (2021).
- [130] V. Dmitrašinović, A. Hosaka, and K. Nagata, *Mod. Phys. Lett. A* **25**, 233 (2010).
- [131] H.-W. Lin, E. R. Nocera, F. Olness, K. Orginos, J. Rojo *et al.*, *Prog. Part. Nucl. Phys.* **100**, 107 (2018).
- [132] R. G. Edwards and B. Joó (SciDAC, LHPC, and UKQCD Collaborations), *Nucl. Phys. B, Proc. Suppl.* **140**, 832 (2005).